Capturing Lasers in a Maritime Environment

by

Midshipman 1/C Warren Rooney

A Capstone Project Report Submitted to the Faculty of
The Weapons and Systems Engineering Department
United States Naval Academy, Annapolis, Maryland

Faculty Advisor: Prof Svetlana Avramov-Zamurovic

Department Chair: Prof Kiriakos Kiriakidis

09MAR15

Contents

Capturing Lasers in a Maritime Environment

Author: Midshipman 1/C Warren Rooney
Contact Information: wwrooney@gmail.com

***Abstract*—As directed energy systems become used more frequently in military operations, the need for detection systems becomes increasingly essential. On axis detection is the easiest method of laser detection, but the practicality of such a system in combat is almost nonexistent. Instead, since lasers scatter due to particles in the atmosphere, a method of off-axis detection is preferred. This paper presents a method to detect lasers from an off-axis position, and to map its trajectory in various environments. This trajectory includes the slope, direction, and approximate source location for the beam.**

INTRODUCTION

Motivation

Lasers are an extremely efficient tool for militaries to use if they are harnessed correctly. Due to the extremely linear nature of the energy propagation, meaning most of the energy travels in the direction the laser is pointed with minimal spreading, lasers can serve very useful roles as a communication tool and as a weapon system. However, lasers also have critical vulnerabilities when it comes to operating in real world environments. Since laser light is both particles and waves of light, it is susceptible to the properties of diffraction and scattering. In a maritime environment, such as the one in which the Navy operates, there are many different particles present in the atmosphere which can interfere with laser propagation. Particles and atmospheric effects such as sea salts, humidity, dust, water particles, and fog all play a role in how a laser interacts with the environment as it propagates. As the laser hits these particles and the energy scatters the overall intensity of the beam deteriorates, but this same scattering effect allows cameras to detect laser light from a position that is not directly in the path of laser propagation called an off-axis angle. This off-axis detection method is extremely important to military application because it means that a detection system could pick up a laser propagating in the environment without having to be in the direct path of the laser.

Problem Statement

This project focused on using the principles of scattering and diffraction to determine the trajectory of a laser beam propagating in a maritime environment. The scattering light can be used to determine slopes of the laser, and the diffraction of the beam can be used to help determine the intensity of the beam as it propagates through the environment. The goal of the project was to use only one camera perspective to gather all of the information necessary to model the laser propagation in three dimensions. In order to model the beam in three dimensions, the project was focused on determining path, direction, and general location of the source. A perspective is defined as a camera location relative to the laser beam as it propagates such as above the beam or to the side of the beam. An illustration of the different kinds of energy present when a laser propagates through an environment is shown in Figure 1.

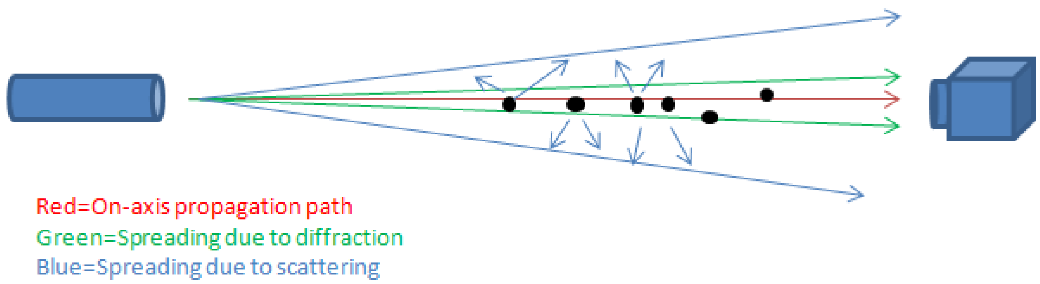

Figure 1 Illustration of the different spreading principles

The project was successful as a reliable method of modeling a laser as it propagates through an environment was produced. This could be extremely useful if expanded upon because it would serve as a foundation for actual implementations to be used on Navy ships to counter hostile laser threats.

Related Work

Determining the effect of laser wavelength to maximize laser efficiency [1]

The paper written by Sprangle, Penano, and Hafizi titled “Optimum Wavelength and Power for Efficient Laser Propagation in Various Atmospheric Environments” discusses the various effects actual maritime environments have on laser propagation in great detail. The lasers examined were high energy lasers because those are the ones that are most important to understand for military applications as weapons. The paper analyzed the effect of hygroscopic aerosols such as sea salt, water, and organic material and non-hygroscopic aerosols such as dust, soot, and other carbon-based compounds. The difference between hygroscopic and non-hygroscopic aerosols is that hygroscopic particles are water soluble while non-hygroscopic are not. Another characteristic of non-hygroscopic particles are that they typically have much higher absorption coefficients than hygroscopic. Scattering and absorption coefficients however, typically tend to rely more on the size of the particles rather than their ability to be water soluble or not. One phenomena that is highly determinant on hygroscopic vs. non-hygroscopic is thermal blooming. Thermal blooming occurs as energy absorbed by aerosols from laser propagation is used to heat and vaporize the particle. These aerosols heat the surrounding air conductively, and thermal blooming occurs. Non-hygroscopic tend to have much higher thermal blooming because they do not vaporize as easily, and thus heat the air much more than hygroscopic particles. This paper also utilized the use of the Advanced Navy Aerosol Model to model the maritime environment near the surface. Lasers with different wavelengths were tested, and the results for three of these are shown in Table 1.

Table 1 Parameters for Three Different Wavelengths (Table 1 is Source [1])

Laser Wavelengths, λ [μm]	1.045, 1.625, 2.141
Laser Power, P_T[MW]	1
Laser Spot size, R_0 [cm]	50
Aperture Diameter, D[cm]	80
Peak Laser Intensity at Source, I[kW/cm^2]	0.27
Average Intensity along Path, $\langle I \rangle$ [kW/cm^2]	2
Pointing Jitter, $\Delta\Theta_{jitter}$ [μ rad]	2
Laser Beam Quality, M^2	4
Range, L[km]	5
Wind Velocity, V_w [m/sec]	5
Turbulence Strength, C_n^2 [$m^{-2/3}$]	10^{-15}
Water Vapor Absorption Coefficient, α_{wv} [km^{-1}]	3×10^{-3}, 2×10^{-3}, 3×10^{-3}
Aerosol Scattering Coefficient, β_A [km^{-1}]	1.2×10^{-1}, 7×10^{-2}, 5×10^{-2}
Aerosol Absorption Coefficient, α_A [km^{-1}]	2×10^{-3}, 2×10^{-3}, 3×10^{-3}
Effective Aerosol Absorption Coefficient, [km^{-1}]	1×10^{-3}

Analysis of long term beam spread and wander for Gaussian beam [2]

The maritime environment introduces many disturbances into the atmosphere which can disrupt the propagation of a laser beam. In order to determine how effective laser propagation will be, it is necessary to evaluate how the aerosols will reduce laser efficiency. The Gaussian beam used in the paper is one in which the intensity distribution is approximated well by Gaussian distribution functions. These beams are ideal for laser testing because they are extremely coherent meaning the majority of the laser energy exits the source traveling in the same direction. This paper introduces a new refractive index power spectrum in order to predict how high humidity atmospheres can detract from laser performance due to scattering and absorption. This power spectrum is useful because it allows for a maritime environment to be characterized prior to laser use. The paper also focuses on beam spreading and beam wandering over long distances. Beam wander occurs when the laser beam spontaneously deviates from its propagation path due to random temperature fluctuations in the atmosphere. Beam spreading occurs due to the diffraction of light as it bends around objects in the atmosphere over the course of its propagation. The combination of these two parameters is called long term beam spreading and it is a useful parameter to determine because it directly affects the intensity profile of the beam throughout its path. The size of the beam at the target can be modeled from these parameters and is shown plotted in Figure 2 from three different power spectrums.

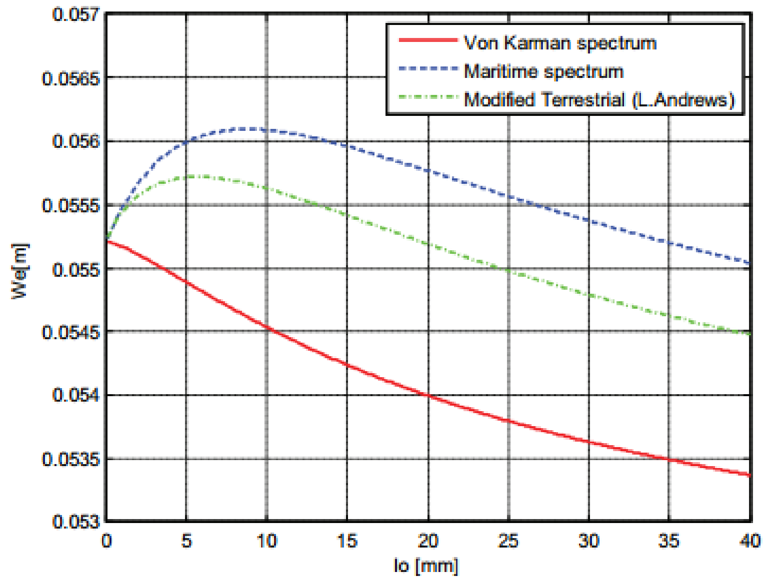

Figure 2 Long Term Beam Spread as a Function of Inner Scale (Figure 3 in Source [2])

The inner scale is caused by a "bump" which is present in the Hill power spectrum and occurs when the inner scale and wavenumber is approximately 1. The paper focuses on this aspect of beam propagation, and chooses to ignore outer scale effects which cause a beam to behave differently by reducing the long term beam spread.

Using partially coherent beams to propagate in random media [3]

One of the issues that arise when trying to propagate a laser in the atmosphere is the random distribution of aerosols. This randomness can lead to significant distortion when a fully coherent beam is propagated through a maritime environment in which many particles are present in the air. The paper by Gbur and Wolf titled "Spreading of partially coherent beams in random media" looks at the potential benefits of propagating partially coherent beams through a medium with many random aerosols rather than using a traditional fully coherent laser. This paper looks to examine the effects of partially coherent beams in a turbulent environment because they argue that minimal work has been done on this issue prior to the paper. Although this project did not utilize partially coherent beams, this paper provides valuable insight into the limitations of fully coherent beams in turbulence as compared to partially coherent beams. The desired results of the paper were to create equations which could be used to model laser behavior in a turbulent environment, and to determine what specific circumstances would lead to partially coherent beams being more effective than fully coherent ones. The paper analyzed both the propagation of a beam through turbulence, and the spreading of the beam through turbulence to analyze the performance of partially coherent beams. In addition to examining the propagation and spreading of the beam, the team also analyzed the range of the beam using various range models such as the Rayleigh range. The Rayleigh range is defined as the distance at which the cross-sectional area of the beam doubles in free space. From their results, they found that two relevant parameters could be used to define how the beam behaved in free space versus a turbulent environment. The first parameter, z_T, was defined as the distance which resulted in a 10% increase in area for the beam in a turbulent atmosphere compared to free space. This parameter was used to measure the beam's overall resistance to turbulence in the atmosphere. The second parameter, R_T, was used to classify beams into two groups. Beams which were affected by turbulent spreading before free-space diffractive spreading were one group, and the other were beams which behaved in the opposite manner. In general, the results showed that partially coherent beams were more resistive to turbulence in the atmosphere. One tradeoff for this performance however, is that partially coherent beams are also prone to a larger angular spread in free-space than fully coherent beams are. This result shows that a decision must be made in determining the ideal laser to use in an environment based off competing interests of trying to minimize diffractive spreading while maximizing turbulence resistivity.

Analyzing the spreading of partially coherent beams in turbulent atmosphere [4]

Another analysis of partially coherent beams involved examining how different modes of coherency for the laser. Again, fully coherent lasers are extremely sensitive to aerosols present in a turbulent environment, and they experience a large amount of scattering as a result. Partially coherent beams remain relatively unaffected by the same turbulence when compared to the performance of fully coherent beams. This paper analyzed partially coherent beams created by using the Gaussian Schell-Model at various modes of decomposition. The results showed that beams with higher-order modes of decay experienced smaller amounts of spreading as compared to lower-order modes. Figure 3 shows an example of the intensity decay for partially coherent beams in comparison with that of the fully coherent beam.

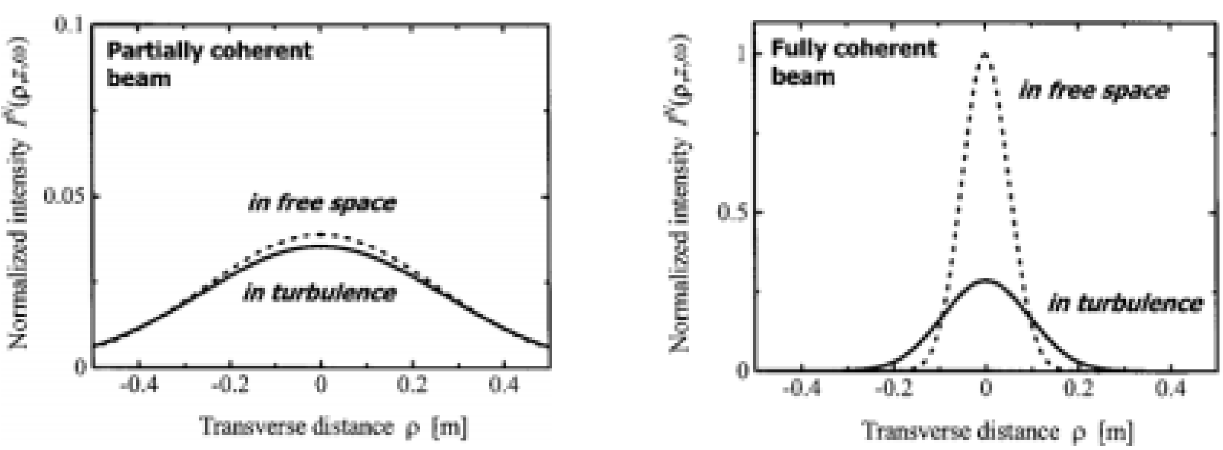

Figure 3 Normalized Intensities for Partially Coherent Beams vs. Fully Coherent Beams (Figure 3 in Source [4])

As can be seen in Figure 3, the partially coherent beam has similar intensity values in both free space and turbulence whereas the fully coherent beam has a significant intensity drop between the two environments. This proves the statement that partially coherent beams are much less affected by turbulence than fully coherent beams are.

Off-axis detection in a maritime environment [5]

There have been multiple papers studying the theory behind off-axis laser detection. One of these studies discusses a model for detecting off-axis scattered light. The model is based behind Mie scattering from aerosols in a maritime environment, and the overall effect on a pulsed laser. Situations in which Mie Scattering can be used often arise when the size of scattering particles is comparable to the wavelength of the light. One of the key aspects of the paper is the work done on the theory behind off-axis scattering. This theory is important to the work in this paper because it provides a baseline for finding the radiance of a beam at a target in plane geometry as shown in Equation 1.

$$\frac{dI(\theta,t)}{d\theta} = P_o[t_{SR}(\theta) - t]\exp[-\alpha(z + r)]\frac{\beta(\theta+\varphi)}{r^2}\frac{dz}{d\theta} \quad (1)$$

A graphic representation of the geometry from which Equation 1 was found is shown in Figure 4.

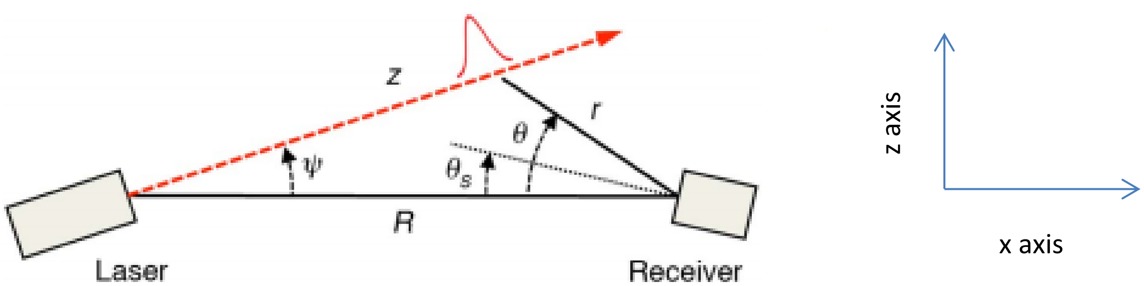

Figure 4 Geometry of off-axis laser detection and coordinate frame

As the picture illustrates, the angle ψ is the angle from the baseline to the laser, θ_s is the angle of a reference direction for the receiver, θ is the angle of the receiver to the laser, z is the distance from the source, R is the distance from the laser to the receiver, and r is the distance the laser travels to the receiver. From the equation, t_{SR} is the propagation time, t is the time, $\frac{dz}{d\theta}$ is the change in z as a function of the change in θ, α is the beam extinction coefficient due to absorption, and β(θ+ψ) is a volume scattering function. This equation is represents the rate of change of intensity as a function of the receiver angle, and the time that has elapsed as shown by the term $\frac{dI(\theta,t)}{d\theta}$. This function is the scattered radiance at the power receiver, and is dependent upon the initial power ($P_o(t)$). It is also important to note that this model utilizes plane geometry which eliminates the requirement to find a third dimension since the laser propagation is aligned along the third axis. Data for the model was gathered over a vast range of distances which extended to approximately 5 km. The tests were conducted using a Ship Board Laser Acquisition System with a horizontal field of view from -45° to 45°. A wide field of view is much more extensive than will be used in the experiments performed in this paper, but it shows the applicability of similar experiments on a larger scale. Also, the atmospheric data during various weather conditions were calculated through the use of the Advanced Navy Aerosol Model. This is a database that was created by the Navy to quantify characteristics of aerosol particles in varying weather conditions.

Design Process

Objectives

The objectives of the project as discussed before focus on attempting to map the trajectory of a laser as it propagates through a maritime environment. The first objective is to successfully replicate the laser's trajectory in three dimensions to within 0.5 cm. For the first set of experiments this is an error of less than 2%, and for the second and third experiments the desired error is less than 0.5%. The second objective is to replicate the trajectory using only one camera perspective with as little variance in the camera position as possible. The third objective is to create application curves based on the laser's intensity both as the camera moves along the laser's propagation and as the camera moves farther away from the laser. The reason for this objective is to use the laser's intensity decline to model the laser's position through the application curves to obtain the third component of the laser's trajectory as will be discussed later. Again, the goal for the accuracy of the application curves is within 0.005 m.

Constraints

The biggest constraints were in relation to the size of the testing environment. For the initial tests in the water tank to simulate the water environment, the size of the compartment was 1.05 m. The size of the second compartment which was used for the atmospheric environment was larger than the first compartment at a size of 1.2 m. Additionally; the camera was limited to a range of approximately 2 m from the compartments since the lab setup was not conducive to larger testing ranges. The laser tests were confined to evening tests in order to minimize the amount of external light interfering with the analysis of the laser. There was also a constraint with the amount of time available to dedicate to the project, and the amount of time needed to gain the necessary background knowledge before beginning tests. The power of the laser was constrained due to safety concerns and was kept to 2 mW in order to minimize the risk for vision damage. All of the tests were also constrained to a laboratory environment and no tests were conducted in the actual environment due to all of the complexities introduced once a real environment is used for testing. There were no real budgetary constraints since there was not a critical need for equipment that was not already present by the laser research team at the Naval Academy.

Functions and Morphological Chart

Table 2-Morphological Chart for Equipment Selection

Functions:	**Possible Means:**			
Laser Power	Class 1	Class 2	Class 3a	Class 3b
Laser Type	HeNe	Laser Pointer		IR Laser
Laser Color	Red	Green		Blue
Detection Method for Beam Analysis	Camera	Point Detector		Camera + Notch Filter
Weather Station for Environmental Modeling	AcuRite	OregonScientific		Weather Channel

Ethical Considerations

There were few ethical factors which played into the decision making throughout the process since the project is being conducted on a small scale, but larger scale implementations could introduce some ethical concerns. To start, the laser power was kept low so there was no concern for any damage that could be done to government property or individuals who were working in the lab. More powerful lasers however, could have enough energy to inadvertently damage property so the location of testing for these lasers would have to be chosen carefully. Additionally, the goal of attempting to detect and plot the trajectory of a laser propagating through the atmosphere does not pose any ethical concerns at its fundamental level. The potential uses for such a technology however, could introduce ethical dilemmas. Since the idea behind the project is for use by the Navy to better identify lasers in a maritime environment, the way in which a system like this could be used must be carefully considered. It would be important to ensure that any system used to detect lasers for the purpose of neutralizing a hostile threat would be used only if a Navy vessel was targeted or a neutral civilian ship was in danger. If such criteria were met, then this project would not be unethical in pursuing.

Engineering Analysis or Simulations

The biggest component of engineering analysis that went into the project was how to use mathematical principles to plot the laser trajectory from the images taken. Since the camera was taking pictures from the side, a slope could be generated by taking the difference between the height values from the start of the image to the end and dividing that by the change in distance values as shown in the example photograph in Figure 5.

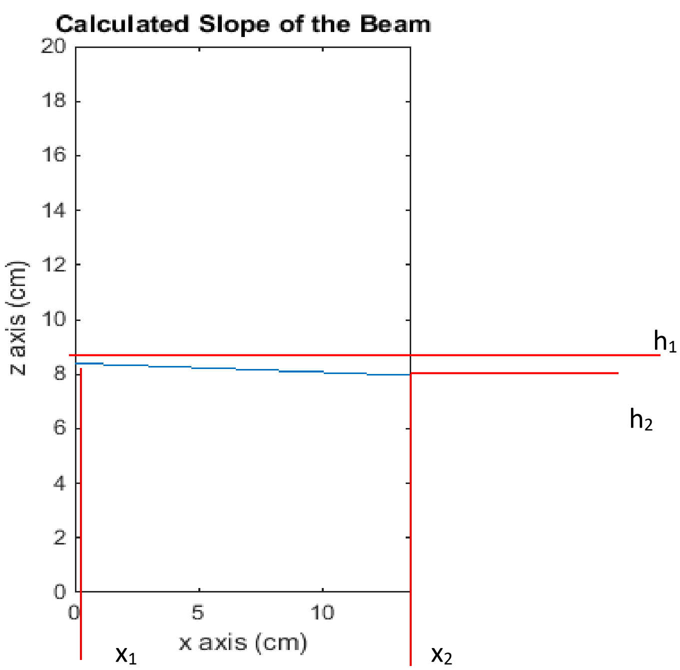

$$\text{slope} = \frac{h_2 - h_1}{x_2 - x_1}$$

Figure 5 Example Calculation of Laser Trajectory Slope

This calculation accounted for two of the three dimensions, but it was necessary to find a way to account for the third dimension without changing the camera perspective. Before the intensity application curves were created, the use of similar angles was employed on the water tank in order to account for the third dimension The idea behind the use of similar angles is that if a line is offset from a perpendicular axis, then the angle necessary to rotate a line in order to align back perpendicularly with the offset line is the same angle of the orginal offset line. This process and how it was used to determine the third dimension of laser trajectory will be discussed in length in the next section, but the principle of similar angles can be illustrated by Figure 6.

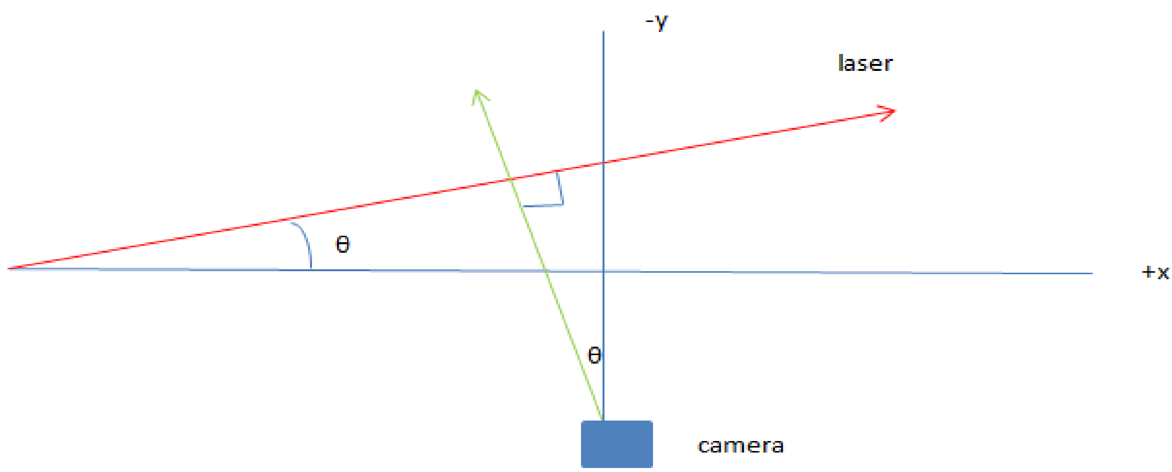

Figure 6 Illustration of the Similar Angle Principle

Component Selection

The components of the project were all chosen to maximize the safety of testing throughout the experimentation. The laser power was chosen to be 2 mW because that would ensure no damage was done to the vision of anyone in the lab and did not require the use of safety goggles. In addition, a red helium-neon (HeNe) laser was chosen because red light has the lowest intensity level, and a HeNe laser provides laser light with the best coherency. The coherency of a laser is defined as the amount of light traveling in the same direction of propagation. Other options such as laser pointers do not provide comparable coherency levels, and a HeNe laser is the best option for experimental testing. The camera used to capture the laser beam was a DCU223M camera developed by THORLABS. This is a CCD camera with a resolution of 1024 x 768 pixels and has a USB 2.0 connection. The DCU223M was chosen because it could be connected directly to a laptop without any external equipment required, and this camera was already available for use because it had been previously purchased. A red notch filter was also added to the camera in order to filter out the light that was not red, and allow for the laser to be easier to identify. The Weather@Home weather station from OrgeonScientific was chosen due to its ability to log pressure, temperature, and humidity and transmit that data wirelessly to a remote receiver. This was a crucial element because it allowed the weather station to remain in the sealed compartment while the date continued to be transmitted about the environment.

Final Design

Research Process

This project was not a traditional Systems capstone in the sense that there was no real design component involved. Instead, this project was focused on research of laser behavior in different maritime environments and determining ways of capturing the laser propagation in order to properly plot its trajectory in space.

Experiment 1: Close Camera Position and Large Camera Displacement

The first experiments that were performed were focused on figuring out how to capture the beam and develop a working program which could take images from the camera and analyze them in order to produce a plot of the laser in space. In the first experiment, as shown by Figure 7, the camera was kept at a constan`t distance of 0.30 m away from the laser propagation and moved along the propagation path. The coordinate frame for the entire experiment is also included in the figure.

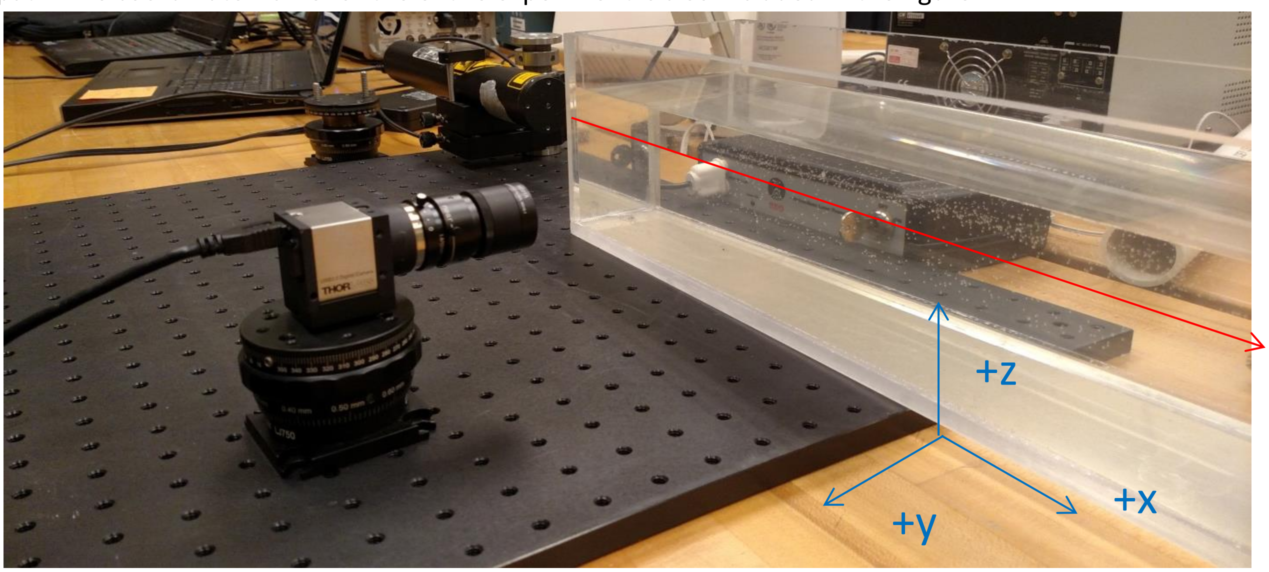

Figure 7 Setup for Initial Experimentation and Coordinate Frame

The camera was moved along the beam's path and three images were taken at 0.36, 0.55, and 0.80 m respectively. These fixed parameters allowed for an algorithm to be developed more easily since there were very few unknowns to account for. This algorithm that was developed is exemplified by the pseudo-code shown in Figure 8, and the full code can be found in Appendix 1.

```
Import 3 photographs from camera

Calculate the intensity of the beam in each image

Convert the intensity images into binary images

      Done by thresholding each image

Plot the original image and binary representation for comparison

Calculate and create a slope for each image

      Uses the 'polyfit' command

Plot the original image and slope calculation for comparison

Average the three slopes for more reliable value

Use similar angles to calculate third dimension

Plot laser trajectory in three dimensions

      Include estimate area of laser source
```

Figure 8 Psuedo-code for Laser Trajectory Algorithm

For each laser image imported, the laser was converted to an intensity image and that same intensity image was then converted into a binary representation. Since the laser intensity diminished as it propagated farther along the water tank, the threshold values had to diminish accordingly. These values were chosen to be 15, 13, and 11 for each of the first, second, and third images respectively. Each binary representation served to eliminate any noise in the images and return positive values for only the laser itself. Slope values could then be calculated from the binary images using the camera height, distance from the laser, pixel size of the DCU223M, and position along the laser's path. Since the testing environment was confined and the source of the laser was readily apparent, the origin was defined as the laser source for the x-axis, the camera location for the y-axis, and the table for the z-axis. Consequently, in every final plot the laser always has a negative y-axis trajectory in relation to the camera. The camera height was measured to be 0.087 m, and this was used to calculate the height of the beam. The field of view for the camera was found to be 29.5° and this was used to plot the overall length of the beam's trajectory in the x-axis. The laser trajectory in the x-z plane was found by using the slope calculations, but since the x-y plane trajectory was completely independent of the slope calculations the similar angle principle could be used. In order to use this principle, the camera was rotated to align perpendicularly with the laser. This angle was recorded and if the camera was rotated clockwise then the angle was positive, but if the rotation was counterclockwise then the angle was negative. The code was found to be successful for any configuration of laser whether it was propagated in a straight line, angled up, down, towards, or away from the camera. Figure 9 shows the different steps of the algorithm while Figure 10 shows the final result alongside the actual test image for a laser which was propagated up and away from the camera.

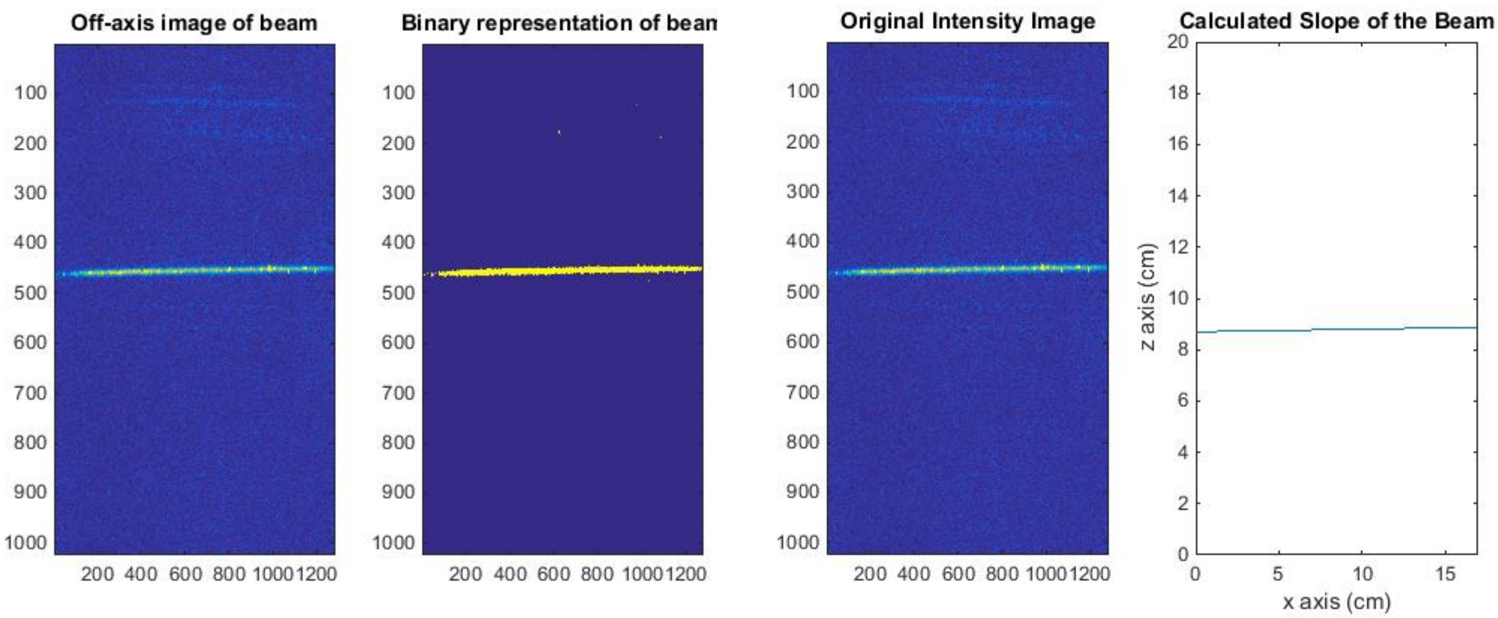

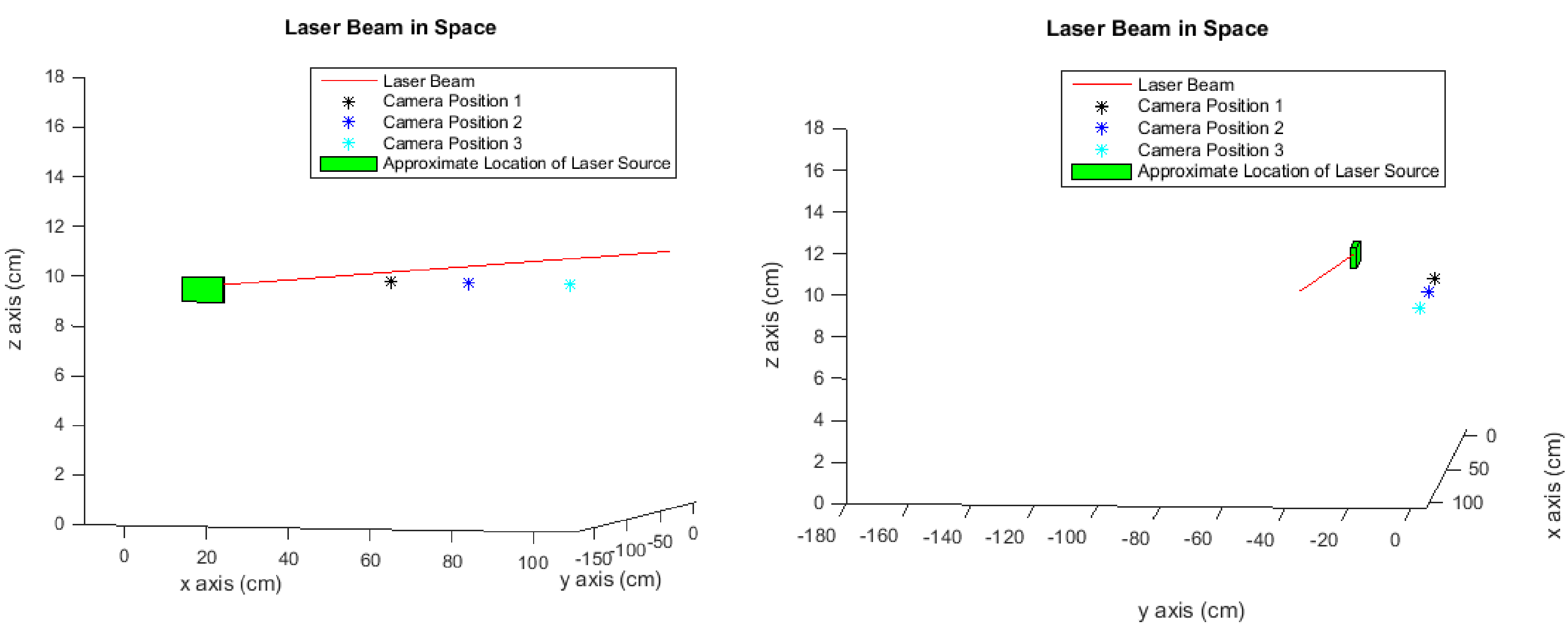

Figure 9 Laser Analysis and Results for Test 1

The plot was found to meet the criteria of being within 0.5 cm compared with the actual measurement. The height of the actual laser was measured to be 10.4 cm at a distance of 0.1 m, while the plot calculated the slope to be 10.2 cm at the same distance meaning the error was 0.7%. Additionally, the beam was measured to have an offset of 4.9 cm from the centerline at 0.1 m, and the plot measured the same distance to have an offset of 5.25 cm with an error of 1.2%. In order to demonstrate the effectiveness of the laser in all situations, another test is included and shown in Figure 10 in which the laser was propagated down and towards the camera.

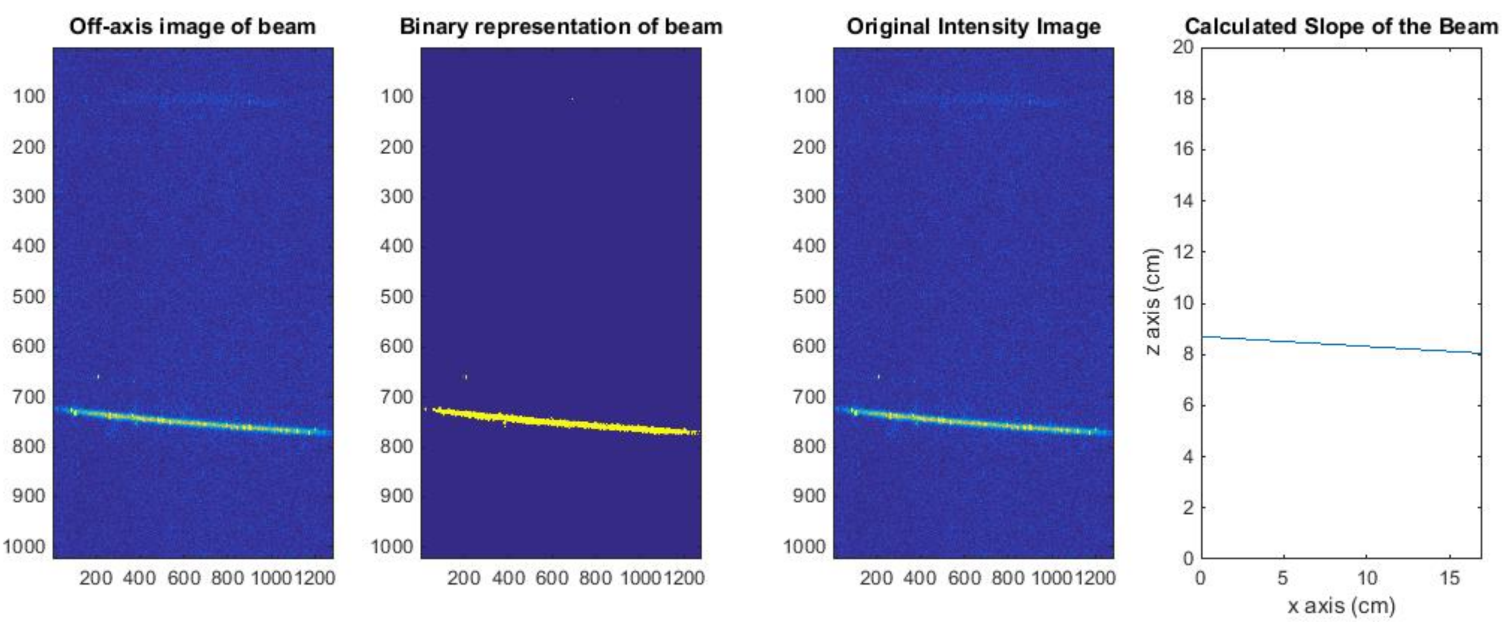

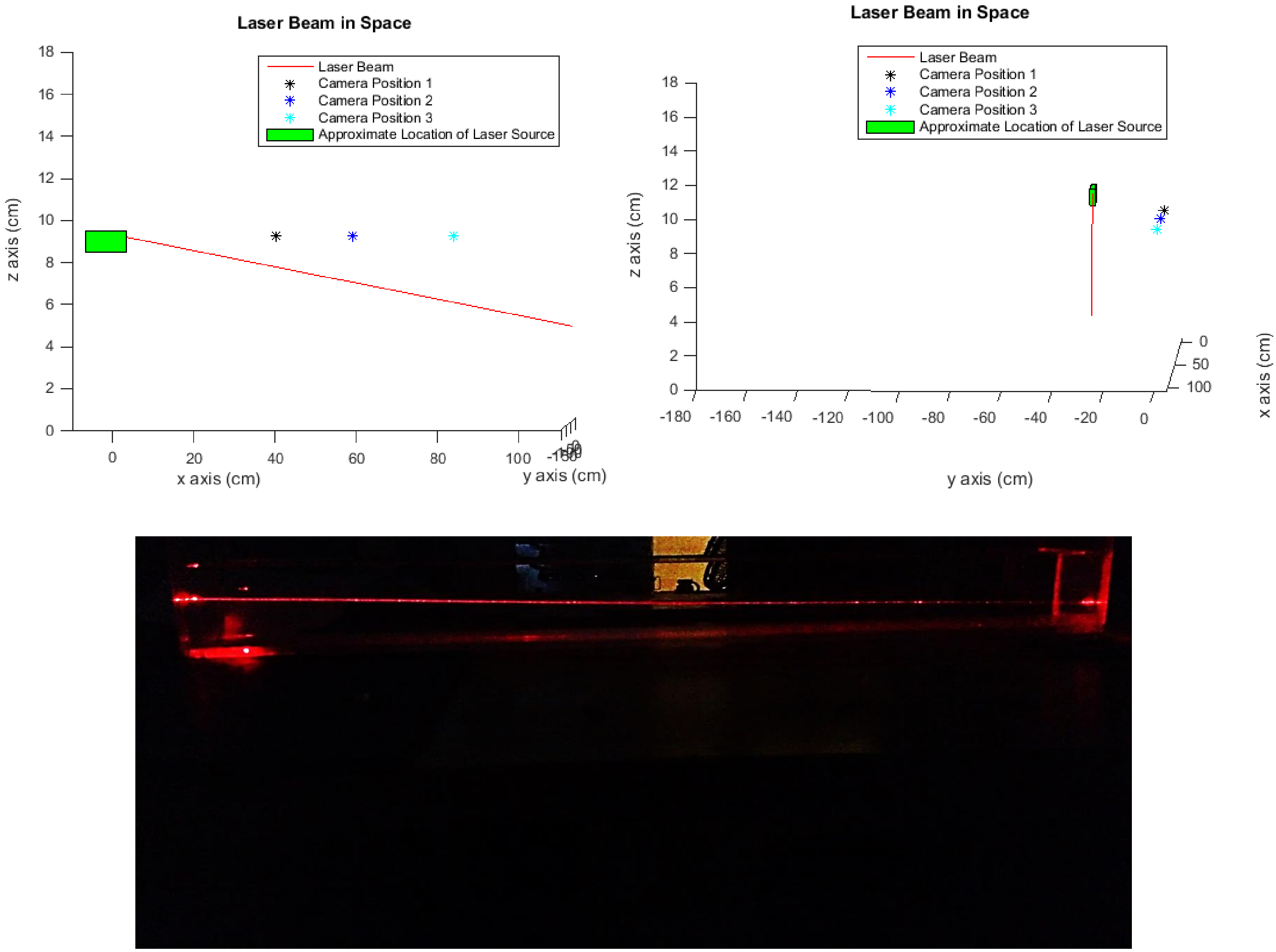

Figure 10 Laser Analysis and Results for Test 2

Once again, the plot and actual measurements were found to be within the criteria of 0.5 cm of each other. At a distance of 0.1 m along the propagation path, the laser was measure to be 4.6 cm high, and the plot of the trajectory calculated the beam to be at 4.85 cm which meant the error was 0.83%. The offset at this distance was measured to be 4.96 cm from the centerline, and the plot calculated the trajectory to have an offset of 5.24 cm which meant the error was 0.93%. Although these measurements are within the performance metrics defined in this project, there is still a consistent source of error of approximately 0.25 cm. This error source most likely arose from errors in the height measurements of the camera, errors in the angle measurement to make the camera perpendicular to the laser, and rounding errors. More precise measuring devices to record heights and angles could lead to more accurate measurements in the plots of trajectory and would help reduce the error.

Experiment 2: Far Camera Distance and Minimal Camera Displacement

Once the algorithm was tested with several different parameters, the initial experimentation was over and the second stage of experimenting began. The goal of this second part of the water tank experiment was to make the situation more realistic. This was accomplished in two ways, the first was to increase the camera distance from the actual beam propagation, and the second was to decrease the amount of distance the camera traveled along the propagation path. This new lab setup would better simulate a camera system which could be placed on a ship, and the setup is shown in Figure 11 from the camera's perspective.

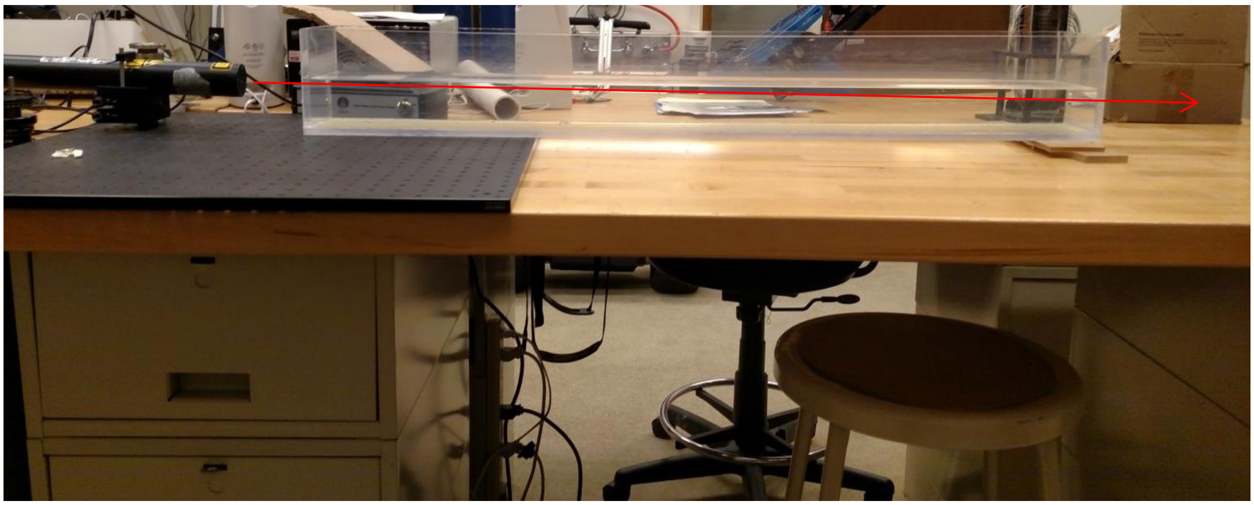

Figure 11 Setup for Second Experiment

The fundamental principles were the same in this test as they were for the initial experiment, but the only difference was the camera distance was moved from 0.30 m to 1.7 m and the distance between photographs was minimized to 0.01 m from approximately 0.20 m. Again, the laser was tested in a situation which it was propagated down and towards the camera. The results are shown in a similar fashion as they were in the previous tests in Figure 12.

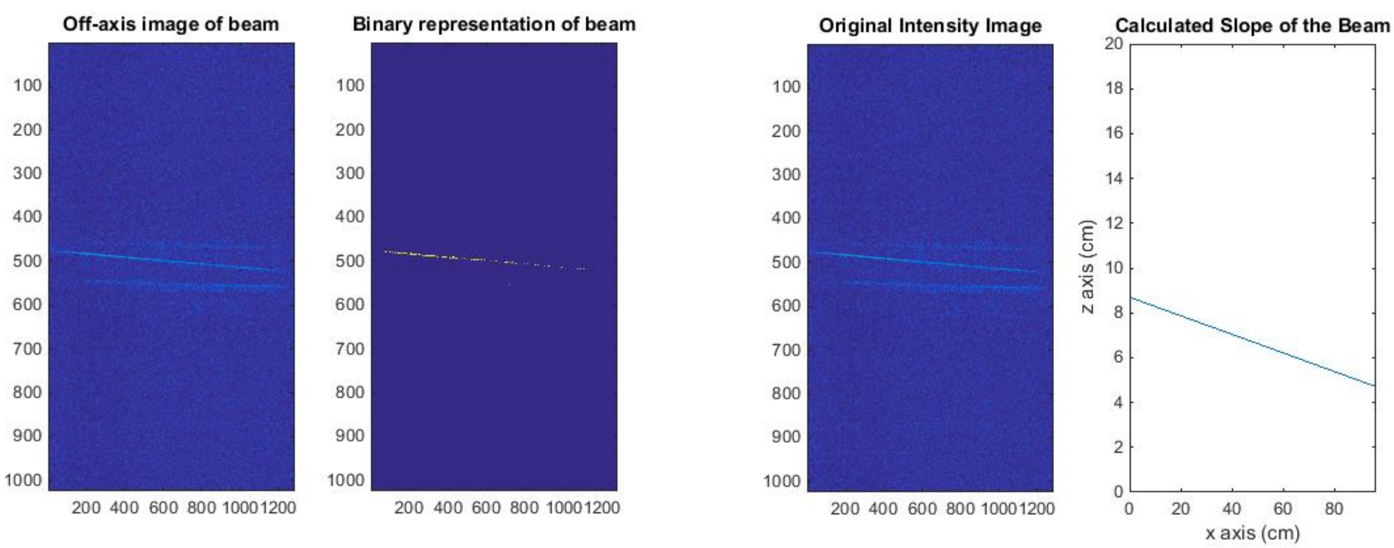

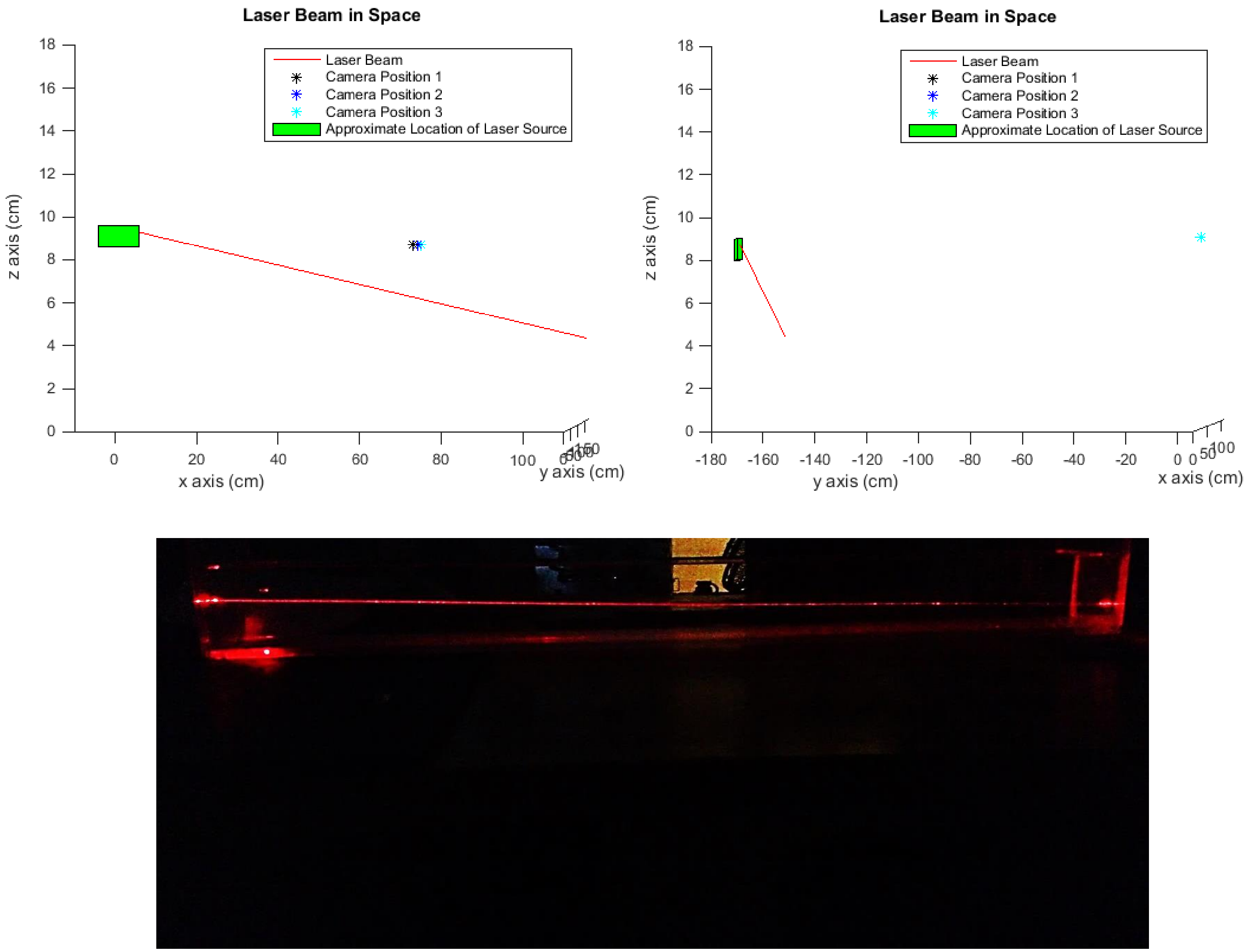

Figure 12 Laser Analysis and Results for Second Experiment

The test at the longer distance had very similar measurements as the second test in the initial experiment with a height measurement of 4.04 cm and offset of 4.9 cm at a distance of 0.1 m with an error of 0.51%. The trajectory plot was almost within the performance metrics once again with a calculated height of 4.26 cm and an offset of 5.2 cm with an error of 0.55%. Although the laser propagation was extremely similar, the y-axis numbers are significantly different as a result of the origin choice. Since the origin of the y-axis was defined as the camera location which is much farther away from the laser source, the y-axis numbers are much more negative but still follow the same trend as before. Although both experiments proved to be successful, this one was much more important because it illustrated the effectiveness of the code at a fundamental level for a larger camera distance.

Experiment 3: Error Measurement for Atmospheric Testing

Once the two experiments were conducted, it concluded the testing in a water tank, and the subsequent tests were conducted in the Compartmentalized Atmospheric Tank (CAT). The CAT was designed as an airtight compartment through which smoke, fog, smog, or any other atmospheric disturbance could be pumped in and the laser could be tested various environments. In order to obtain qualitative data for each test, the Weather@Home Multi Channel Sensor from Oregon Scientific was intended to be used to log pressure, temperature, and humidity data. Unfortunately, the Weather@Home sensor was not available for use as it was delayed in ordering, therefore the experiment did not log the changing atmospheric conditions. The new setup for testing required the laser to be attached to the CAT in order to create an airtight seal which further reduced the testing distance, but did not make a significant impact in the various tests. The CAT and laser for the new experimental setup are shown in Figure 13.

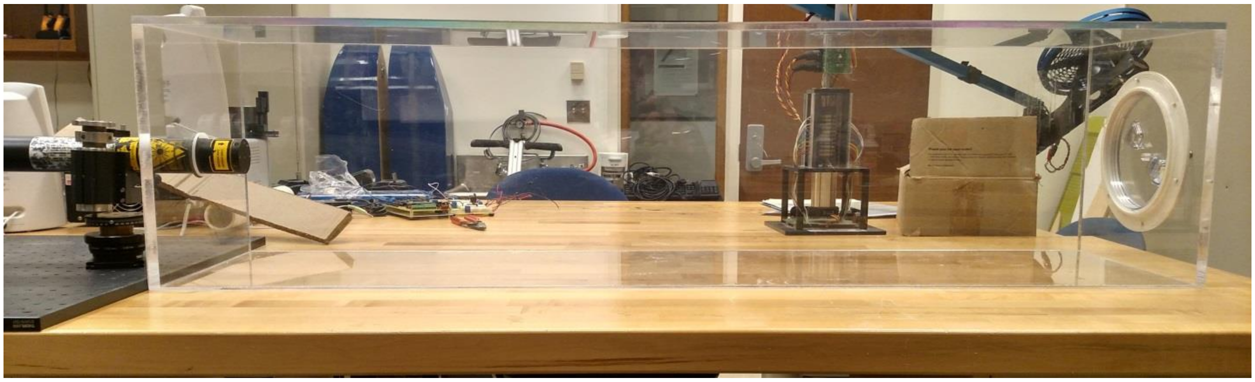

Figure 13 Setup for CAT Experiments

The experiment was set up to take measurements at 0.44, 0.45, and 0.46 m along the beam's propagation path at distances of 1.6 and 1.8 m. The goal of the experiment was to determine how much error existed in the program to model the laser if the distance was measured incorrectly. Figure 14 shows the laser experiment taken from a distance of 1.6 m.

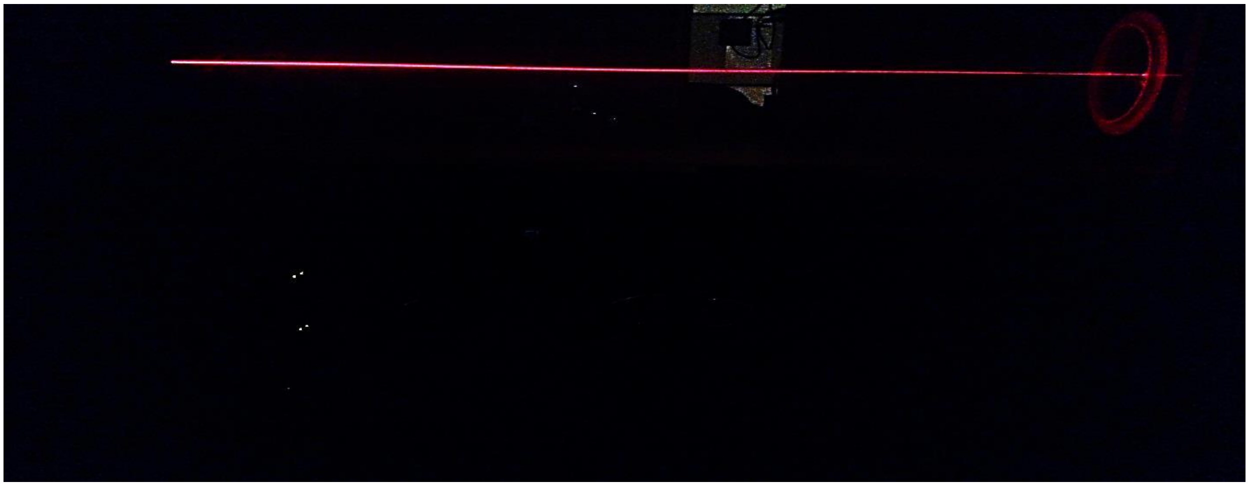

Figure 14 CAT Experiment at a distance of 1.6 m

The height of the laser was measured to be 0.149 m at a distance of 0.75 m along its propagation path. Once the actual height was measured, the code was run at a distance of 1.6 and 1.8 m to determine what the computed height was. The final results of the code at 1.6 and 1.8 m are shown from left to right respectively in Figure 15.

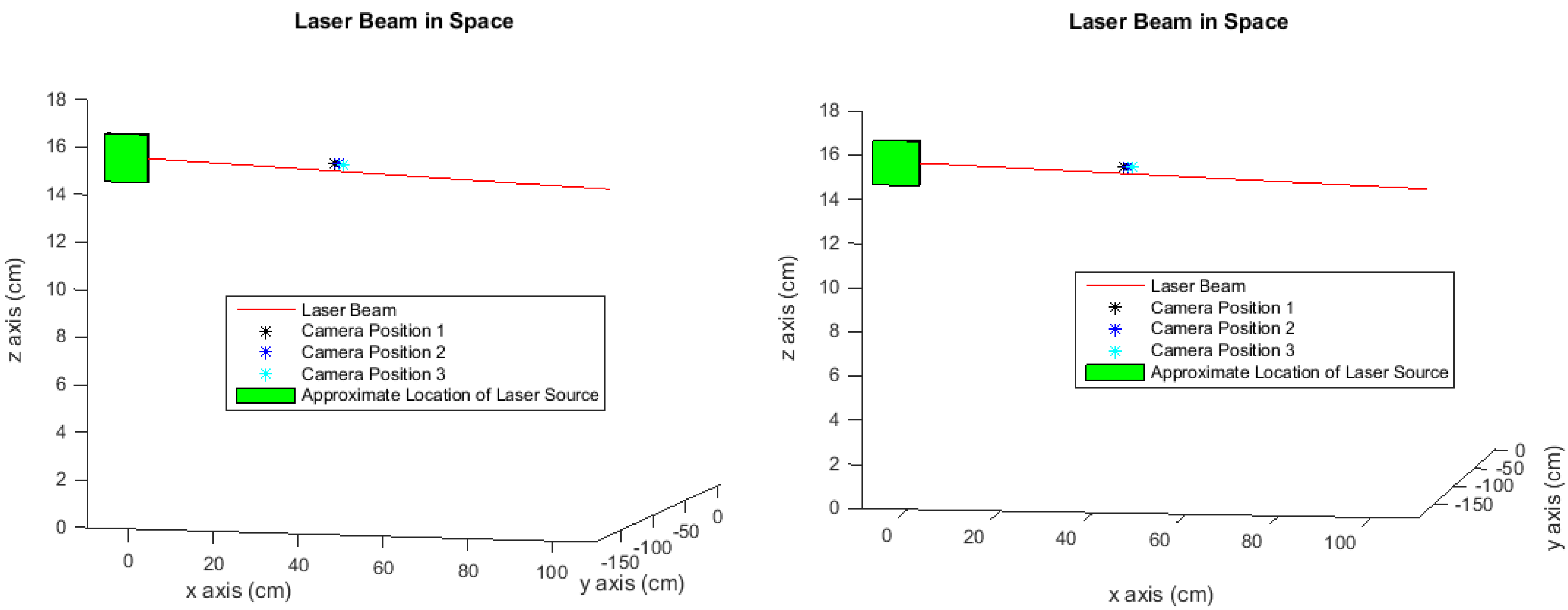

Figure 15 Laser Analysis Results at 1.6 and 1.8 m

As can be seen from the image, the two results were extremely similar with the results at 1.6 m reading 0.1474 m and 0.1475 m at 1.8 m. The resulting error values for these two tests were then computed to be 0.083% and 0.089% respectively. However, to determine the effectiveness of the code in a real situation the error values for the different readings were calculated for a distance of 1 km by using the values at 1.6 and 1.8 m using a proportion. When the distance was theoretically increased to 1 km, the resulting error for the test at 1.6 m was found to be 100 m and 83.33 m for the test at 1.8 m. Not only were the differences in errors 17 m apart, but the absolute error of 100 m and 83.33 m illustrates that the code would not be very effective at long range. These error values prove that the code would need revision in order to improve accuracy, and also demonstrate the need for a more precise system of measuring distances than relying on a meter stick to measure heights and distances when the need for absolute precision is necessary.

Results and Analysis

Demonstration Plan

The verification of the algorithm to plot the trajectory of the laser propagation in space is not dynamic and thus does not require much equipment. A ruler for smaller measurements and a meter stick for larger measurements are all that is required. For the first two experiments, once the laser is oriented in whatever arbitrary direction is desired several measurements can be taken. These measurements should be spread over multiple distances, and can include both heights of the laser and offset from original source location. These measurements can then be used to verify the accuracy of the program by comparing the measured results to the ones created by the program.

Performance Measures

As mentioned before, the project was not dynamic in nature, and thus there were not many performance measures to be used. The most concrete performance measure to evaluate how successful the project was involved measuring the difference between actual distances and heights with those produced by the algorithm. The goal was to create results that were accurate to within 0.5 cm for the different laser tests. For all of the tests conducted, the results from the calculated trajectory plots were within the threshold for success as compared to the actual measurements. As was discussed before, the consistent source of error most likely arose from precision errors when determining the height of the camera and angle of camera rotation, which directly influenced the calculations for the trajectory plot. With more precise readings, this error would most likely be decreased even further.

Project Management

Life Long Learning

Throughout the process of this research there were many things learned that would be beneficial in future work and research regarding engineering problems. The first was how to work independently, and how to figure out a system to do so efficiently. When performing independent research, it is extremely important to have clear goals and to be able to self-motivate in order to reach those goals because there is no one around to really keep you accountable besides your advisor. In addition to the overall process of independent research, there was an immense amount of learning done in regards to lasers and how they operate. A great deal of background knowledge was necessary in order to attempt to solve this problem, and through this process many previously unknown attributes of lasers were learned. The basic properties of diffraction and scattering were known from basic Physics courses, but how the laser interacts with the environment, how many different properties can affect laser propagation, the importance of coherency in lasers, and the relative difficulty in capturing laser propagation and then modeling it were all things that had to be learned. Lastly, the endless cycle of trial and error that represents research taught valuable lessons throughout the project. Learning how to critically and creatively think about problems to solve them was extremely vital to the success of this project. The best representation of this came about when trying to solve for the third dimension of laser propagation when initially only the slope information was available. If a solution had not been developed for this, then the project would have been a failure and a significantly less amount of progress would have been accomplished.

Cost analysis and Parts List

PERSONNEL and Equipment	HOURS/AMOUNT	SALARY PER HOUR/COST	TOTAL SALARY
MIDN 1/C Rooney	140	$40	$5,600
Professor Avramov	28	$50	$1,400
Weather Station	1	$40	$40
TOTAL			$7,240

Parts List:

Water Tank

CAT

2 mW HeNe Laser

DCU223M Camera

Red Notch Filter

Laptop

Timeline

The original timeline for this project is as follows:

1. Geometric and Trigonometric Equations (4 weeks)

- Utilize one camera perspective (either from side or above)
- Determine how changing camera angle affects image
  - Relative beam slope as seen by camera
- Find feasibility of solving for laser origin from multiple images
  - Utilize one perspective

2. Laser Testing in Lab Environment (7 weeks)

- Determine power vs. distance relationships
  - As laser propagates through the gas container
  - As camera increases distance from container
- Determine slope of beam from multiple photographs
  - Utilize one camera perspective
- Graph beam and estimated laser origin position
  - Use slope information
  - Use power vs. distance application curves
  - Compare computed results to actual test conditions

3. Laser Testing in Actual Environment (3 weeks if time permits)

- Become introduced with factors necessary to account for in actual atmosphere
  - Ambient light
  - Varying weather conditions
  - Lack of controlled testing environment
- Attempt to capture beam in environment
- Attempt to map beam in similar fashion as lab environment
  - Use slope information
  - Use power vs. distance application curves

4. Compile Final Project Report (14 weeks as goals accomplished)

- Document results from experiments
- Save and document MATLAB code
- Include background information from whitepapers already read

The actual timeline for this project is as follows:

1. Geometric and Trigonometric Equations (4 weeks)

- Utilize one camera perspective (either from side or above)
- Determine how changing camera angle affects image
  - Relative beam slope as seen by camera
- Find feasibility of solving for laser origin from multiple images
  - Utilize one perspective

2. Laser Testing in Lab Environment (10 weeks)

- Determine slope of beam from multiple photographs
  - Utilize one camera perspective
  - Minimize variation in camera location
- Graph beam and estimated laser origin position
  - Use slope information
  - Compare computed results to actual test conditions

3. Compile Final Project Report (14 weeks as goals accomplished)

- Document results from experiments
- Save and document MATLAB code
- Include background information from whitepapers already read

Discussion and Conclusion

This project was successful in computing the general location of the laser source as well as the direction and slope of the laser for small distances. The initial experiment demonstrated the effectiveness of the code in a static maritime environment at a close distance from the laser propagation. As the distance was increased to over 1 m in the second experiment, the code developed proved to be accurate for this distance as well. The third and final experiment however, demonstrated that although the code for analyzing the laser was relatively successful at close distances, there was still variation if the distance from the laser was measured incorrectly. Additionally, when the distance was extrapolated to a realistic distance of 1 km, the errors were shown to be much larger than they appeared in the two previous experiments. With error values of over 50 m, this code was shown to be an ineffective means to quantify the laser's trajectory and potential source location at distances greater than what could be tested in the lab. One recommendation for future projects would be to implement the weather station in later experiments in order to obtain quantifiable data on the changing environmental conditions as different atmospheres are tested. Another recommendation would be to obtain a relationship between the observed intensity of the beam vs. distance along its propagation path for various camera distances. This relationship could then be used as a more reliable means for calculating and modeling the laser's trajectory in the x-y plane instead of relying on relative angles. A third and final recommendation would be to refine the way in which the camera height and distances are calculated. Ideally, a code would be developed in which these values were not necessary, but a more precise means of measurement is vital in codes which utilize these values. Overall, the project was considered successful as the code was able to provide a relatively accurate foundation for finding a laser and source from one camera perspective which can be modified and built upon in later years.

Acknowledgment

I would like to thank Professor Avramov as well as Stephen Guth for working with me throughout the year, helping me with any issues I had with the equipment, and keeping me motivated when I found myself to be off track. Additionally, I would like to thank all the WSE Lab Technicians for helping me through technical difficulties as well as ordering the parts I needed in an expedient manner. Without all these people this project would not have been as successful as it was.

References

[1] Sprangle, Phillip, Joseph Penano and Bahman Hafizi. *Optimum Wavelength and Power for Efficient Laser Propagation in Various Atmospheric Environments*. Washington, DC, 25 October 2005. Journal. <http://oai.dtic.mil/oai/oai?verb=getRecord&metadataPrefix=html&identifier=ADA441474>.W.-

[2] Toselli, Italo, Brij Agrawal and Sergio Restaino. "Gaussian beam propagation in maritime atmospheric turbulence: long term beam spread and wander analysis." *Proceedings of SPIE, the International Society for Optical Engineering* (2010): 78140R-1-10. Electronic.

[3] Gbur, Greg and Emil Wolf. "Spreading of partially coherent beams in random media." *Journal of the Optical Society of America* (2002): 1592-1598. Electronic. <http://www.opticsinfobase.org/josaa/abstract.cfm?uri=josaa-20-6-1094>

[4] Shirai, Tomohiro, Aristide Dogariu and Emil Wolf. "Mode analysis of spreading of partially coherent beams propagating through atmospheric turbulence." *Journal of the Optical Society of America* (2003): 1094-1102. Electronic. <http://www.opticsinfobase.org/josaa/abstract.cfm?uri=josaa-20-6-1094>
[5] Hanson, Frank, et al. "Off-axis detection and characterization of laser beams in the maritime atmosphere." *Applied Optics* (2011): 3050-56.

Appendix 1: MATLAB Code for Laser Analysis

```
%% Slope Experiment Code - Spring
% MIDN 1/C Warren Rooney

%Import all the photos and convert to uint8
[slope1]=uigetfile('*.jpg','Please select which photo you want');%pick
slope1=imread(slope1);
[slope2]=uigetfile('*.jpg','Please select which photo you want');%a
slope2=imread(slope2);
[slope3]=uigetfile('*.jpg','Please select which photo you want');%series
slope3=imread(slope3);

%Determine intensity of the beam
Islope1=.2989*slope1(:,:,1)+.587*slope1(:,:,2)+.114*slope1(:,:,3);
Islope2=.2989*slope2(:,:,1)+.587*slope2(:,:,2)+.114*slope2(:,:,3);
Islope3=.2989*slope3(:,:,1)+.587*slope3(:,:,2)+.114*slope3(:,:,3);

%Convert Images to Binary
[r, c]=size(Islope1);
Islope1bin=Islope1;
for i=1:r
    for j=1:c
        if Islope1(i,j)<15
            Islope1bin(i,j)=0;
        else
            Islope1bin(i,j)=255;
        end
    end
end

Islope2bin=Islope2;
for i=1:r
    for j=1:c
        if Islope2bin(i,j)<13
            Islope2bin(i,j)=0;
        else
            Islope2bin(i,j)=255;
        end
    end
end

Islope3bin=Islope3;
for i=1:r
    for j=1:c
```

```
        if Islope3bin(i,j)<11
            Islope3bin(i,j)=0;
        else
            Islope3bin(i,j)=255;
        end
    end
end

figure(1)
subplot(1,2,1)
image(Islope1)
title('Off-axis image of beam')
subplot(1,2,2)
image(Islope1bin)
title('Binary representation of beam')

figure(2)
subplot(1,2,1)
image(Islope2)
title('Off-axis image of beam')
subplot(1,2,2)
image(Islope2bin)
title('Binary representation of beam')

figure(3)
subplot(1,2,1)
image(Islope3)
title('Off-axis image of beam')
subplot(1,2,2)
image(Islope3bin)
title('Binary representation of beam')

%Create slope of beam
camheight=8.7; %remains constant
dist= 170; %distance of camera to beam in cm
width=dist*tand(29.5); %width of picture in cm
pos1= 73; %36; %camera positions along beam propagation
pos2= 74; %55;
pos3= 75; %80;
x=0:.1:width;

[z1,x1]=find(Islope1bin);
p1=polyfit(x1,z1,1);
b1=(540-p1(2))*4.65e-6+camheight;
%z_1=p1(1).*x+b1; %level slope uncomment
z_1=-p1(1).*x+b1; %+/- slope uncomment

[z2,x2]=find(Islope2bin);
p2=polyfit(x2,z2,1);
b2=(540-p2(2))*4.65e-6+camheight;
%z_2=p2(1).*x+b2; %level slope uncomment
z_2=-p2(1).*x+b2; %-/+ slope uncomment

[z3,x3]=find(Islope3bin);
```

```
p3=polyfit(x3,z3,1);
b3=(540-p3(2))*4.65e-6+camheight;
%z_3=p3(1).*x+b3; %level slope uncomment
z_3=-p3(1).*x+b3; %+/- slope uncomment

figure(4)
hold on
subplot(1,2,1)
image(Islope1)
title('Original Intensity Image');
subplot(1,2,2)
plot(x,z_1)
title('Calculated Slope of the Beam');
xlabel('x axis (cm)');
ylabel('z axis (cm)');
axis([0 width 0 20]);

figure(5)
hold on
subplot(1,2,1)
image(Islope2)
title('Original Intensity Image');
subplot(1,2,2)
plot(x,z_2)
title('Calculated Slope of the Beam');
xlabel('x axis (cm)');
ylabel('z axis (cm)');
axis([0 width 0 20]);

figure(6)
hold on
subplot(1,2,1)
image(Islope3)
title('Original Intensity Image');
subplot(1,2,2)
plot(x,z_3)
title('Calculated Slope of the Beam');
xlabel('x axis (cm)');
ylabel('z axis (cm)');
axis([0 width 0 20]);

%Compute Slope of Beam from 3 Images
%p_beam=(p1(1)+p2(1)+p3(1))/3; %overall slope, level slope uncomment
p_beam=(-p1(1)-p2(1)-p3(1))/3; %overall slope of beam, +/- slope uncomment
b_beam=(b1+b2+b3)/3; %y-intercept of beam
x_beam=0:.1:110;  %distance of beam path
z_beam=p_beam.*x_beam+b_beam;

% figure(7)  %used for initial testing but not needed once code finalized
% plot(x_beam,z_beam);
% title('Path of Beam');
% ylabel('z-axis');
% xlabel('x-axis');
% axis([0 110 0 20]);
```

```
%Calculate Third Dimension of Path
angle=3; %angle of camera rotation to form right angle with beam +=r/-=l
y_beam=x_beam.*tand(angle)-dist; %Origin of y-axis at laser source

%Create 3-D Plot
figure(7)
hold on
plot3(x_beam,y_beam,z_beam,'r');
plot3(pos1,0,camheight,'k*');
plot3(pos2,0,camheight,'b*');
plot3(pos3,0,camheight,'c*');
fill3([0 0 0 0 0],[-dist-1 -dist-1 -dist+1 -dist+1 -dist-1],...
    [8 9 9 8 8],'g');
fill3([-10 -10 -10 -10 -10],[-dist-1 -dist-1 -dist+1 -dist+1 -dist-1],...
    [8 9 9 8 8],'g');
fill3([0 -10 -10 0 0],[-dist-1 -dist-1 -dist+1 -dist+1 -dist-1],...
    [9 9 9 9 9],'g');
fill3([0 -10 -10 0 0],[-dist-1 -dist-1 -dist+1 -dist+1 -dist-1],...
    [8 8 8 8 8],'g');
fill3([0 0 -10 -10 0],[-dist-1 -dist-1 -dist-1 -dist-1 -dist-1],...
    [8 9 9 8 8],'g');
fill3([0 0 -10 -10 0],[-dist+1 -dist+1 -dist+1 -dist+1 -dist+1],...
    [8 9 9 8 8],'g');
title('Laser Beam in Space')
xlabel('x axis (cm)');
ylabel('y axis (cm)');
zlabel('z axis (cm)');
legend('Laser Beam','Camera Position 1', 'Camera Position 2',...
    'Camera Position 3','Approximate Location of Laser Source');
axis([-10 110 -180 5 0 18]);
```